Chinese Chemical Letters 33 (2022) 4549–4558

Contents lists available at ScienceDirect

Chinese Chemical Letters

journal homepage: www.elsevier.com/locate/cclet

Transition-metal-catalyzed switchable divergent cycloaddition of *para*-quinone methides and vinylethylene carbonates: Access to different sized medium-sized heterocycles

Junwei Wang[a,1], Lei Zhao[a,1], Chen Zhu[b,1], Ben Ma[a], Xiaolong Xie[a], Jian Liu[a], Shiyun He[a], Magnus Rueping[b,*], Kun Zhao[c,*], Lihong Hu[a,*]

[a] *Jiangsu Key Laboratory for Functional Substances of Chinese Medicine, School of Pharmacy, Nanjing University of Chinese Medicine, Nanjing 210023, China*
[b] *KAUST Catalysis Center (KCC), King Abdullah University of Science and Technology (KAUST), Thuwal 23955-6900, Saudi Arabia*
[c] *Department of Medicinal Chemistry, Key Laboratory of Chemical Biology, School of Pharmacy, Cheeloo College of Medicine, Shandong University, Ji'nan 250012, China*

ARTICLE INFO

Article history:
Received 8 November 2021
Revised 19 January 2022
Accepted 23 January 2022
Available online 31 January 2022

Keywords:
Medium-sized rings
Divergent cycloaddition
Regioselectivity
para-Quinone methides
Vinylethylene carbonates

ABSTRACT

Divergent synthesis of medium-sized rings with controllable ring sizes represents a longstanding challenge in organic synthesis. Herein, we developed a transition-metal-catalyzed switchable divergent cycloaddition of *para*-quinone methides and vinylethylene carbonates by controlling the steric hindrance of substituent. Different from reported alkoxide-triggered annulations, this process undergoes a regiodivergent allylation of *para*-quinone methides followed by 1,6-addition reaction, providing a new route to selectively synthesize seven- to ten-membered nitrogen-containing heterocycles in high yields with excellent regioselectivities. This protocol features a broad substrate scope, wide functional group tolerance as well as operational simplicity. The reaction mechanism was investigated by conducting a series of control experiments as well as DFT calculations and the origins of the regioselectivities of the cycloaddition process were rationalized.

Medium-sized rings (MSRs, 7–11 members), in particular N- and O-containing heterocycles, frequently appear in a wide range of bioactive natural products and pharmaceuticals [1,2]. Among them, benzo-fused medium-ring heterocycles have gained increasing attention recently because of their potential pharmaceutical values (Scheme 1a) [3–5]. However, the efficient construction of medium-sized heterocycles presents a formidable challenge in organic synthesis due to their inherent entropic factors and unfavorable transannular interactions [6]. Although a number of synthetic strategies have been reported to prepare medium-sized rings, including ring-closing metathesis [7–9], metal- and organo-catalyzed cyclization reactions [10–13] and so on [14,15]. Most established methods are only suitable for the synthesis of certain sized heterocycles, changing the size of the ring usually requires designing new methods and substrates, which is quite costly and inefficient. Therefore, it is highly desirable to develop a unified approach for divergent synthesis of medium-sized heterocycles with various ring sizes. To date, no divergent [4 + *n*] cycloaddition reactions (n = 3–6) have yet been documented. To fill this gap, we sought to develop a highly efficient divergent cycloaddition reaction to selectively construct seven-to ten-membered heterocycles.

Over the past decade, vinylethylene carbonates (VECs) have arisen as versatile precursors for Pd-containing dipole synthons in organic synthesis [16–18]. Typically, in the presence of palladium catalysts, VECs could generate zwitterionic π-allyl palladium species or palladacyclic intermediates *via* a decarboxylation process (Scheme 1b). The research groups of Kleij, Zhang and others have demonstrated that a wide range of nucleophiles could attack the terminal (C5) [19–26] or internal (C3) [27–29] position of Pd-π-allyl species to deliver linear or branched building blocks in high efficiency. Furthermore, applications of VECs in [3 + 2] or [5 + *n*] cycloaddition reactions to construct five-membered heterocycles [30–35] or MSRs [35–40] have also been well studied. Recently, Zhao and co-workers found that VECs could be used as a reaction switch for divergent cycloadditions. In 2017, they disclosed the first [5 + 4]/[3 + 2] cycloaddition of VECs and azadienes, affording benzofuran-fused nine-membered heterocycles and five-membered spirocyclic products, where VECs were served as

* Corresponding authors.
E-mail addresses: magnus.rueping@kaust.edu.sa (M. Rueping), kzhao2013@sdu.edu.cn (K. Zhao), lhhu@njucm.edu.cn (L. Hu).
[1] These authors contributed equally to this work.

https://doi.org/10.1016/j.cclet.2022.01.063
1001-8417/

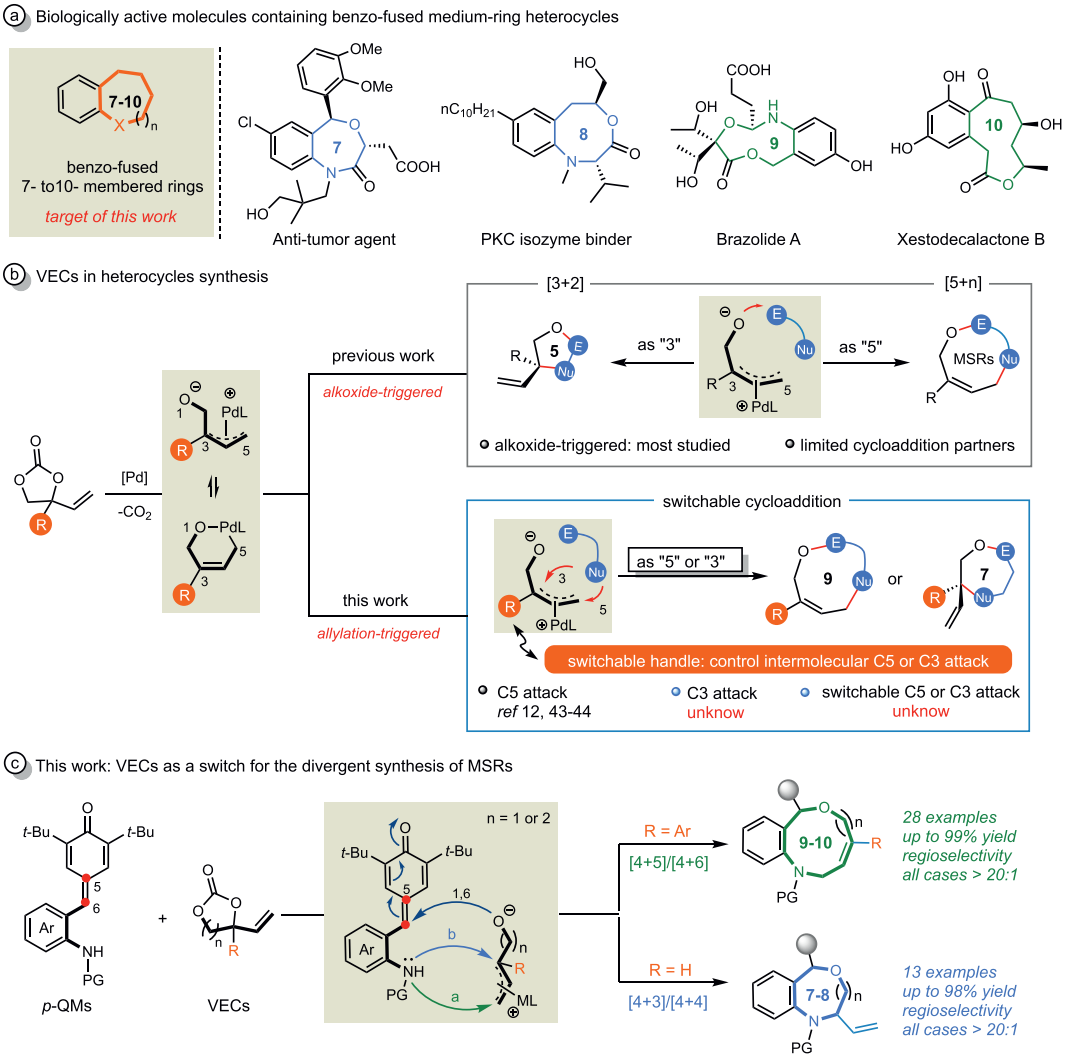

Scheme 1. Profile of VECs-involved cycloaddition reactions and our synthetic strategy.

"5" or "3" synthon and the steric hindrance played an important role in the switch of the regioselectivity [41]. Quite recently, they reported a divergent [4 + 2]/[3 + 2] cycloadditions of VECs and azadienes, and an unprecedented switch from alkoxide-π-allyl to dienolate reactivity was achieved by the use of palladium-titanium relay catalysis in this case [42].

Despite the progress made, most cycloaddition reactions of VECs were based on an alkoxide-triggered annulation process (Scheme 1b, top), the intermolecular allylation-triggered annulations have been less explored (Scheme 1b, bottom) [12,43,44]. To the best of our knowledge, reactions relied on allylation-triggered processes, in which nucleophiles selectively reacted with C3 or C5 of π-allyl species followed by intramolecular annulations, are still unknown to date (Scheme 1b, bottom). Therefore, further application of VECs in novel reactions beyond oxygen anions-triggered cycloadditions for the construction of different sized MSRs skeleton is highly warranted.

Stimulated by pioneering studies of VECs and our ongoing research efforts on *para*-quinone methides (*p*-QMs) [45–54], we were attracted to the cycloaddition of *ortho*-tosylaminophenyl-substituted *p*-QMs and VECs. We envisioned that the annulation reaction between *p*-QMs and VECs should proceed in a cascade fashion, in which the sulfonamide motif would firstly attack on the terminal or internal position of Pd-π-allyl intermediates in a controllable manner followed by an intramolecular 1,6-addition reaction to deliver the [4 + 5] or [4 + 3] cycloaddition adducts respectively (Scheme 1c).

To test the feasibility of this intriguing hypothesis, we chose *p*-QM **1a** and phenyl VEC **2a** as the model substrates to optimize the reaction conditions (Table 1). Initially, we carried out the screening of different bases in the presence of $Pd(PPh_3)_4$ (entries 1–6). First, several commonly used organic bases were evaluated, but the results were disappointing (entries 1–4). To our delight when DBU was employed, the expected reaction occurred, affording desired [4 + 5] adduct **3a** in 66% yield with high regioselectivity, and no [4 + 3] adduct **4a** was observed (entries 5 and 6). Encouraged by this result, another palladium precursor and more phosphine ligands were screened (entries 7–10), and it turned out that the combination of $Pd_2(dba)_3{\cdot}CHCl_3$ and dppe ligand significantly improved the efficiency of this reaction (91% yield, entry 10). Next, the influence of solvent was examined, however, other solvents (*e.g.*, DCE, $CHCl_3$, THF, acetone and acetonitrile) failed to give better results (entries 11–15). With the optimal solvent, the reaction temperature was further examined (entries 16–18) and we found that 60 °C was the appropriate temperature. After establishing the optimal base, catalyst and solvent, other reaction parameters such as the catalyst/ligand loading were finally examined (entries 19–21). We were pleased to find that a simple cocktail containing

Table 1
Optimization of the reaction conditions.[a]

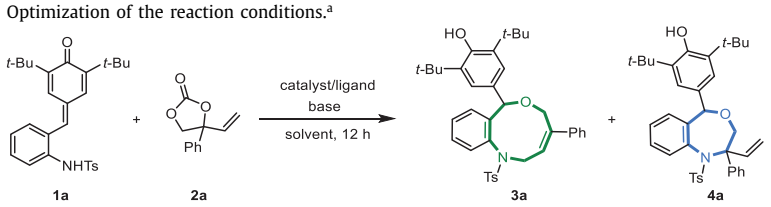

Entry	Catalyst	Ligand	Base	Solvent	T (°C)	Yield of **3a** (%)[b]
1	$Pd(PPh_3)_4$	–	Et_3N	Toluene	60	0
2	$Pd(PPh_3)_4$	–	DIPEA	Toluene	60	0
3	$Pd(PPh_3)_4$	–	DMAP	Toluene	60	Trace
4	$Pd(PPh_3)_4$	–	DABCO	Toluene	60	Trace
5	$Pd(PPh_3)_4$	–	Cs_2CO_3	Toluene	60	43
6	$Pd(PPh_3)_4$	–	DBU	Toluene	60	66
7	$Pd_2(dba)_3$•$CHCl_3$	PPh_3	DBU	Toluene	60	60
8	$Pd_2(dba)_3$•$CHCl_3$	dppp	DBU	Toluene	60	67
9	$Pd_2(dba)_3$•$CHCl_3$	dppbz	DBU	Toluene	60	74
10	$Pd_2(dba)_3$•$CHCl_3$	dppe	DBU	Toluene	60	91
11	$Pd_2(dba)_3$•$CHCl_3$	dppe	DBU	DCE	60	83
12	$Pd_2(dba)_3$•$CHCl_3$	dppe	DBU	$CHCl_3$	60	26
13	$Pd_2(dba)_3$•$CHCl_3$	dppe	DBU	THF	60	52
14	$Pd_2(dba)_3$•$CHCl_3$	dppe	DBU	Acetone	60	24
15	$Pd_2(dba)_3$•$CHCl_3$	dppe	DBU	Acetonitrile	60	48
16	$Pd_2(dba)_3$•$CHCl_3$	dppe	DBU	Toluene	20	35
17	$Pd_2(dba)_3$•$CHCl_3$	dppe	DBU	Toluene	40	76
18	$Pd_2(dba)_3$•$CHCl_3$	dppe	DBU	Toluene	80	90
19	$Pd_2(dba)_3$•$CHCl_3$(5 mol%)	dppe (10 mol%)	DBU	Toluene	60	97 (95)[c]
20	$Pd_2(dba)_3$•$CHCl_3$(5 mol%)	dppe (10 mol%)	DBU (1.5 equiv)	Toluene	60	57
21	$Pd_2(dba)_3$•$CHCl_3$ (5 mol%)	dppe (10 mol%)	DBU (1.0 equiv)	Toluene	60	48

[a] Reaction conditions: **1a** (0.10 mmol), **2a** (0.15 mmol), catalyst (2.5 mol%), ligand (5.0 mol%), base (2.0 equiv.), solvent (1.5 mL), 12 h.
[b] Yield was determined by ^{1}H NMR with 1,3,5-trimethoxybenzene as an internal standard.
[c] Yield of isolated compound **3a** after chromatography, 4a was not observed.

$Pd_2(dba)_3$•$CHCl_3$ (5 mol%), dppe (10 mol%), and DBU in toluene at 60 °C served as the best reaction conditions, and the expected product **3a** could be isolated in an excellent yield (95%, entry 19).

After establishing the optimized conditions for the synthesis of nine-membered rings, we began to evaluate the generality of this protocol. First, the substrate scope of *p*-QMs part was explored (Scheme 2, top). It was found that *p*-QMs bearing different substituents on the benzene ring could be smoothly converted into the expected nine-membered heterocycles **3a**-**3i** in high yields (74%–99%) and regioselectivities, and the reaction efficiency was less affected by the electronic properties or the position of substituents. The benzene sulfonyl protective group on the nitrogen atom of *p*-QMs also did not affect the efficiency of this reaction, and the corresponding products **3j**-**3l** were obtained in 81%–90% yields. When the benzene sulfonyl protective group was replaced with the methyl sulfonyl protective group, the yield of **3m** was reduced to 47%. Subsequently, the scope of VECs **2** was investigated by varying the substituents on the benzene ring or the size of the R group of phenyl VECs (Scheme 2, bottom). We were pleased to find that various *para*-, *meta*-, or *ortho*-substituents with both electron-rich and electron-poor character on the benzene ring of VECs were well-tolerated, and the corresponding products **3n**-**3v** were delivered in excellent yields (70%–99%). Moreover naphthyl- and heteroarene-substituted VECs could also readily take part in this [4 + 5] annulation reaction, affording desired products **3w** and **3x** in 76% and 57% yield, respectively.

Notably, when aryl groups were replaced by ethylene or alkyl substituents, the corresponding products **3y**-**3aa** were obtained in lower yields (9%–34%). Those results indicated that the reaction efficiency was influenced by the substituent of VECs. We decided to further decrease the steric hindrance of the substituent. Non-bulky substituted-VEC **2a'** (R = H) was synthesized and exposed to the optimal conditions. To our surprise, the nine-membered product **3ab** was not formed and a seven-membered ring product **5a** was isolated, albeit with low yield (20%). In this case the regioselectivity of this annulation process was completely switched, and the sulfonamide species firstly attacked the C3 position of the Pd-π-allyl intermediate forming a kinetically favored seven-membered-ring structure.

Striving for higher efficiency of this [4 + 3] cycloaddition reaction, an optimization study was carried out (see Supporting information for optimization details). We evaluated a range of phosphine ligands, metal catalysts as well as several bases, among which the combination of $[Ir(cod)Cl]_2$ and DABCO was proved to be the optimal reaction choice. Under this condition, [4 + 3] cycloaddition adduct **5a** was isolated in an excellent yield (95%) with high diastereoselectivity (> 20:1). With the optimal conditions in hand, the generality of this [4 + 3] cycloaddition reaction was further explored. As shown in Scheme 3, the substrate scope of this [4 + 3] annulation proved to be very broad as well, a wide range of *p*-QMs **1** bearing electron-rich or electron-poor groups at different position of the benzene ring readily reacted with VEC **2a'** to afford expected seven-membered ring products **5a**-**5h** in high yields and diastereoselectivity. In addition, *p*-QMs **1** with different *N*-protecting groups were also suitable substrates for this transformation, giving corresponding products **5i**-**5l** in 83%–98% yields. The structure and relative configuration of **3a** and **5a** were unambiguously determined by the single-crystal X-ray diffraction analysis, and the structures of other nine- and seven-membered products were assigned by analogy.

To evaluate the robustness and practicality of this novel protocol. A scale-up reaction was performed under the standard conditions. As shown in Scheme 4a, both [4 + 5] and [4 + 3] annulation reactions worked very well on 1 mmol scale, and the corresponding products **3a** and **5a** could be isolated in 93% and 94% yields, respectively. To illustrate the versatility of products, we turned our attention to the exploration of selective transformation of those cycloadditions adducts. To our delight, in the presence of PtO_2 cat-

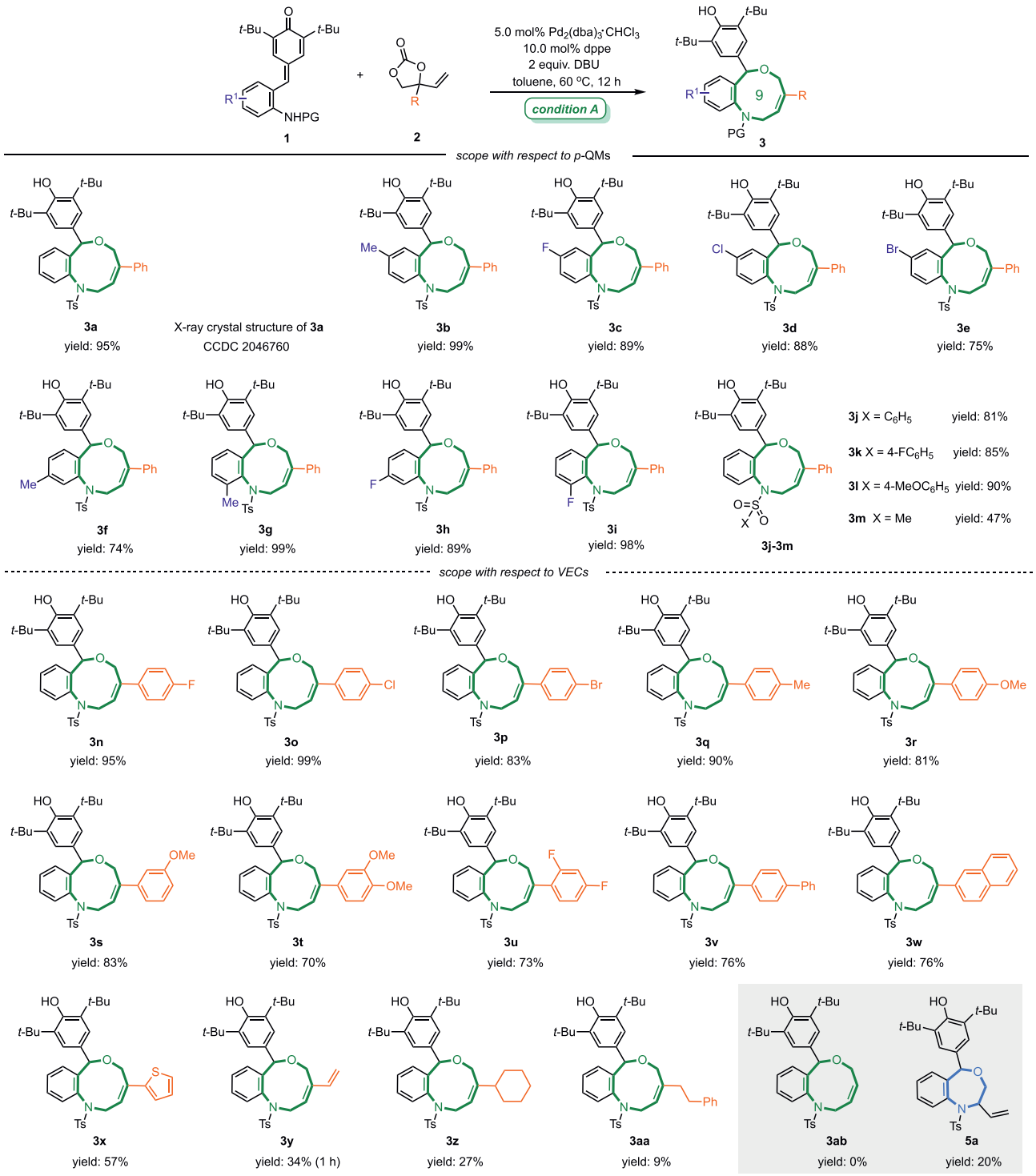

Scheme 2. Substrate scope of the [4 + 5] cycloaddition reaction. Unless noted otherwise, the reaction was performed under condition A: **1** (0.10 mmol), **2** (0.15 mmol), $Pd_2(dba)_3$•$CHCl_3$ (5.0 mol%), dppe (10.0 mol%), DBU (2.0 equiv.), toluene (1.5 mL), 60 °C, 12 h. Yields of isolated products.

alytic hydrogenation of the olefin moiety of **3a** afforded hydrogenated product **6** in 55% yield. Treating with *m*-CPBA diastereoselective epoxidation of **3a** yielded epoxide **7** in a good yield (73%) with high diastereoselectivity (>20:1) (Scheme 4b, top). The Heck reaction of **5a** with idobenzene gave styrene derivative **8** in satisfied results (71% yield; > 20:1 dr). Seven-membered adduct **5a** could undergo olefin metathesis in the presence of Grubbs **II** catalyst, giving the corresponding product **9** with an acceptable yield and good diastereoselectivity (Scheme 4b, bottom).

Next, we turned to explore the enantioselective version of this reaction. As demonstrated in Scheme 5a, a large number of common chiral phosphine ligands were screened, however, only a moderate enantioselectivity was achieved and compound **3a** was isolated with 73:27 er (see Supporting information for more details). In addition, we extended this divergent cycloaddition strategy to the reaction between **1a** and six-membered vinyl carbonate **10**, assembling ten- and eight-membered heterocycles **11** and **12** in satisfying yields and excellent regioselectivity (Scheme 5b). The

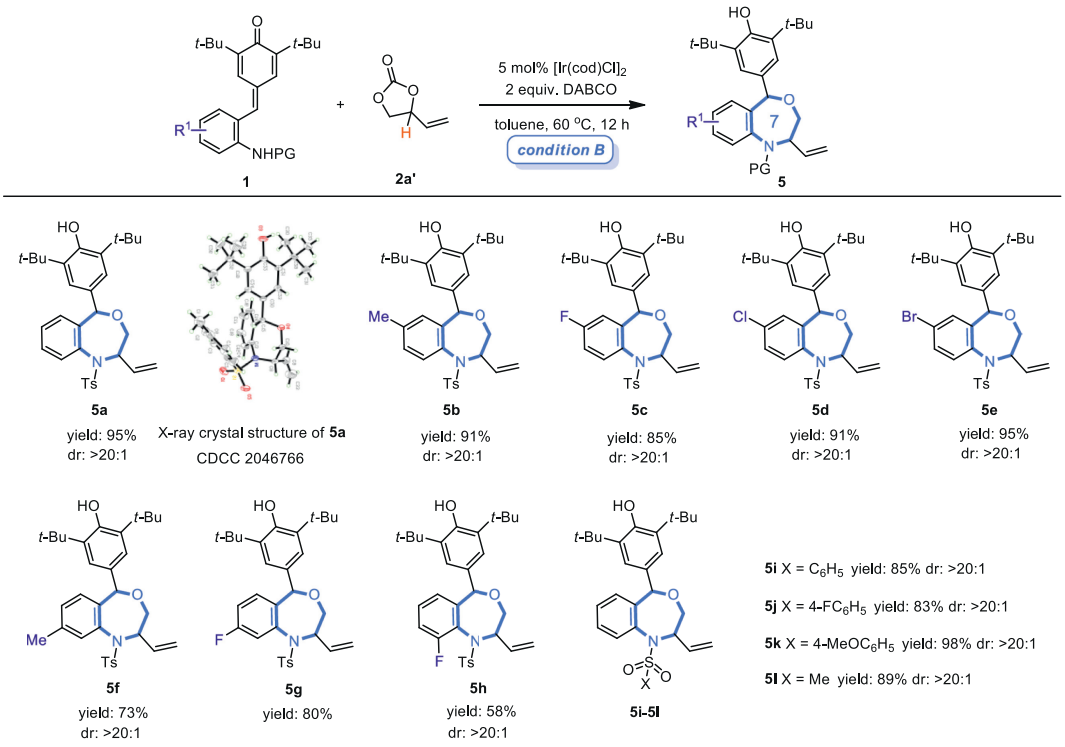

Scheme 3. Substrate scope of the [4 + 3] cycloaddition reaction. Unless noted otherwise, the reaction was performed under condition B: **1** (0.10 mmol), **2a'** (0.15 mmol), $[Ir(cod)Cl]_2$ (5.0 mol%), DABCO (2.0 equiv.), toluene (1.5 mL), 60 °C, 12 h. Yields of isolated products.

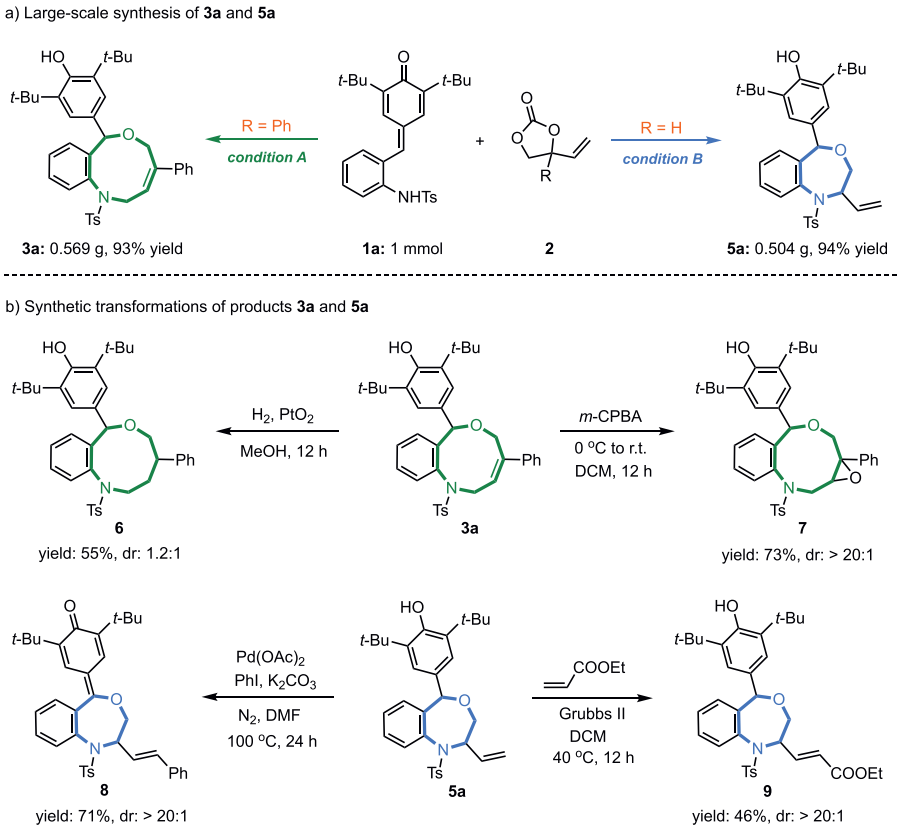

Scheme 4. Scale-up preparation and synthetic applications.

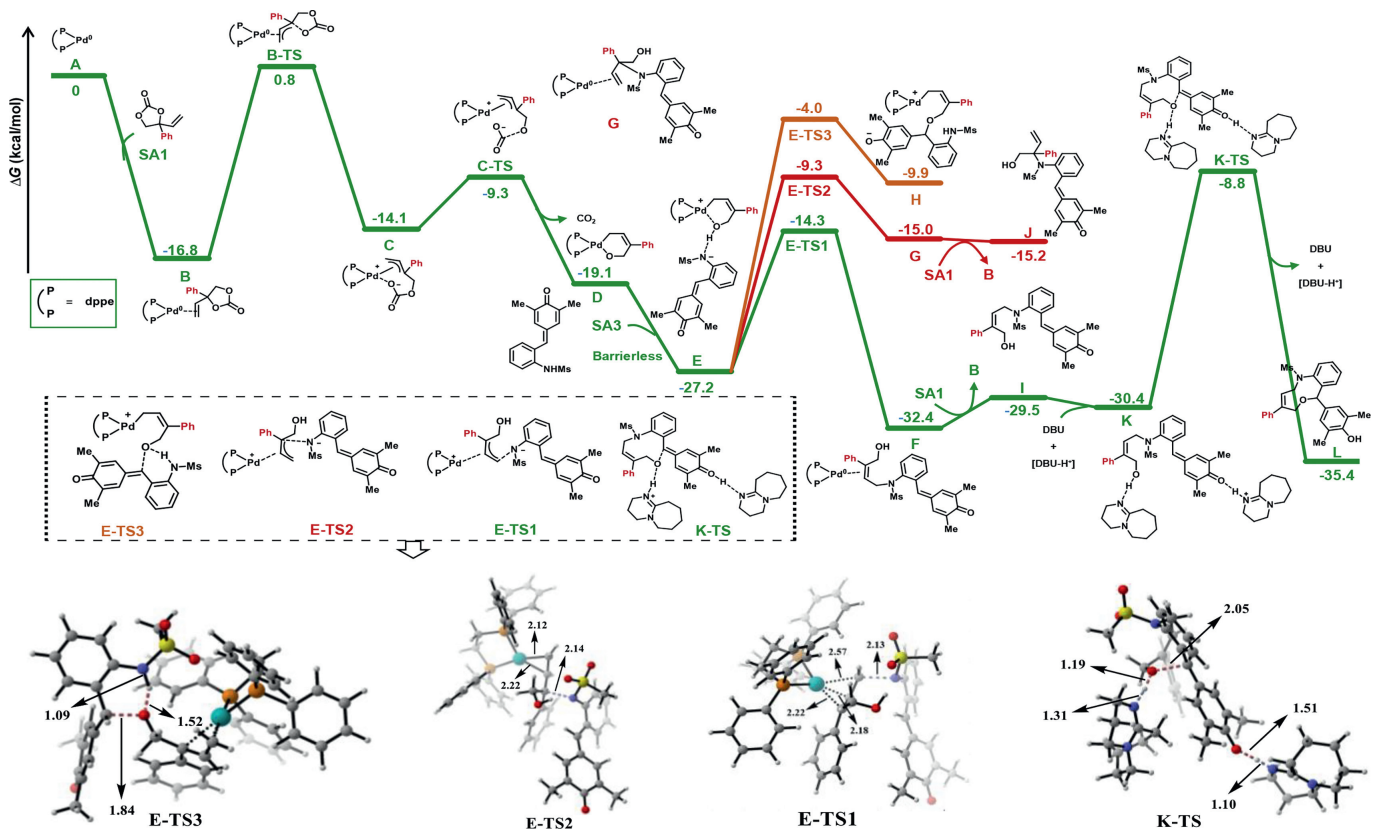

Fig. 1. DFT-computed energy profiles for the [4 + 5] cycloaddition of **SA3** and **SA1**. Free energies in solution (in kcal/mol) at the SMD(toluene)-M06/Def2-TZVPP//PBE/SDD(Pd)/Def2-SVP (other atoms) level are displayed. DFT optimized geometries of selected transition states are shown. Bond lengths are in Å.

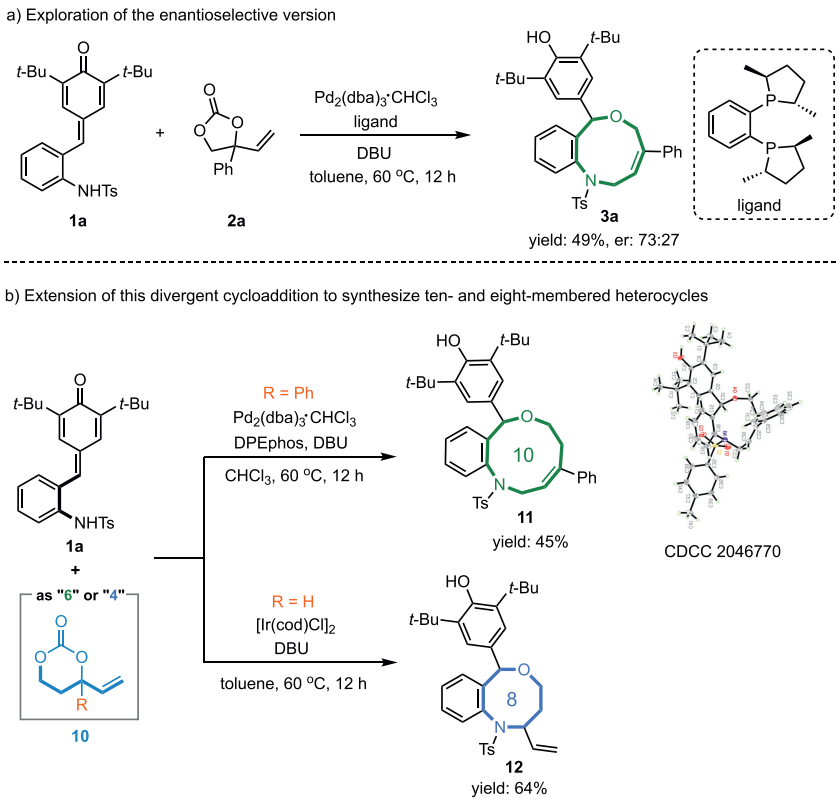

Scheme 5. Extension of this divergent cycloaddition.

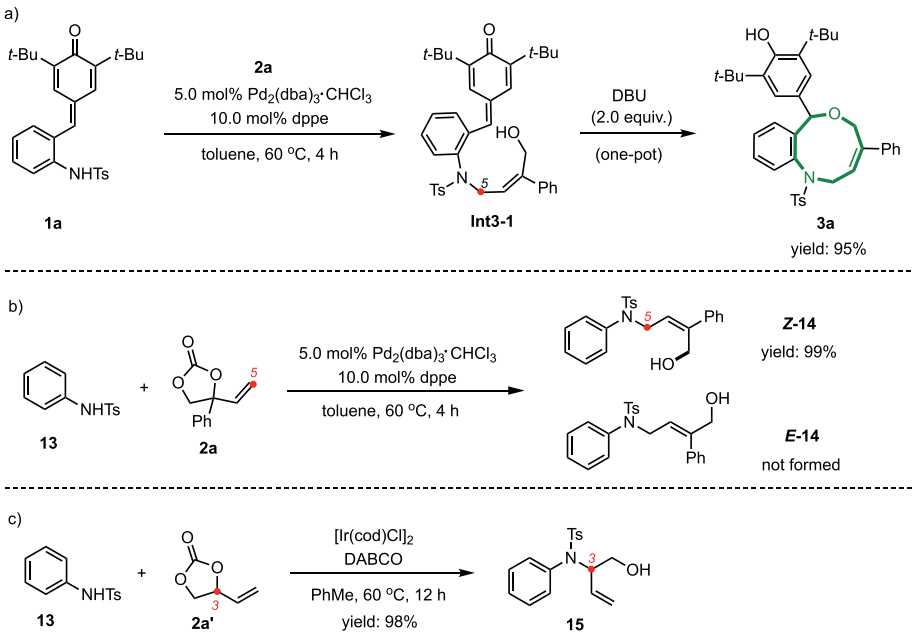

Scheme 6. Control experiments.

structure of the ten-membered heterocycle **11** was unambiguously assigned by the single-crystal X-ray diffraction analysis.

Besides the substrate scope of this reaction, we were also interested in the mechanism of this switchable process. In order to probe the reaction pathway, some preliminary control experiments were conducted. As shown in Scheme 6a, the reaction of *p*-QM **1a** with phenyl VEC **2a** under standard conditions (without DBU) was carried out, and we obtained an uncyclic compound **Int3–1** rather than the cyclic product **3a**. After subsequently adding DBU, the final product **3a** could be afforded in high yield (95%). This result indicated that the overall process was trigged by an intermolecular alkylation of sulfonamides, and then an intramolecular 1,6-conjugate addition reaction occurred to deliver the final cycloaddition adducts. In order to study selectivity issues (terminal versus internal attack, *E- versus Z*-selectivity), we performed a reaction between simplified substrate **13** and phenyl VEC **2a** under standard conditions, and the terminal-attacked product **11** was isolated in high yield as well as with excellent *Z*-selectivity (Scheme 6b); in contrast when the unsubstituted-VEC **2a'** was used, a high C3-selectivity was achieved and the corresponding branched product **15** was obtained in quantitative yield (Scheme 6c).

Finishing those control experiments, a computational investigation by density functional theory (DFT) was undertaken to better understand the details of the whole process, specifically elucidating the origin of the observed regioselectivity of the reaction. All calculations were performed at the SMD(toluene)-M06/Def2-TZVPP//PBE/SDD(Pd)/Def2-SVP (other atoms) level of theory [55–62], and the computational details are given in Supporting information. First, a simplified variant of *p*-QMs **SA3** (*t*-Bu and Ts groups were replaced with Me groups) and phenyl substituted VEC **SA1** were chosen as model substrates to study the energy profile for the [4 + 5] cycloaddition reaction (Fig. 1). The reaction starts with the oxidative cleavage of phenyl substituted VEC **SA1** by the active catalyst, Pd^0(dppe) (**A**), which proceeds *via* adduct **B** and transition state **B-TS**. This cleavage step has an energy barrier of 17.6 kcal/mol. The resulting intermediate **C** has an η^3-allylic group with an open carbonate. Next, a facile decarboxylation of the open carbonate from the intermediate **C** gives the six-membered palladacyclic intermediate **D** *via* the transition state C-TS with only 4.8 kcal/mol energy barrier. In the next step, the *p*-QM **SA3** transfers a proton to the anionic oxygen center of **D**. This process is barrierless, and the generated intermediate **E** is 8.1 kcal/mol more stable. Starting from the intermediate **E**, the energy barriers of three possible nucleophilic attacks were calculated. Both the terminal C5 position and internal C3 position can be nucleophilically attacked by the anionic nitrogen from **SA3**. The attack on the terminal C5 position has the lowest energy barrier of 12.9 kcal/mol (transition state **E-TS1**), while the barrier for the internal C3 position attack is 5 kcal/mol higher (transition state **E-TS2**). The regioselectivity is determined from this terminal nucleophilic attack step. In addition, the third reaction possibility that the nucleophilic attack of the anionic oxygen on the *p*-QM **SA3** was also proved to be less favored, with the highest activation barrier of 23.2 kcal/mol. This result is consistent with the experimental result (Scheme 6a). To push the reaction forward, in the presence of DBU the hydroxyl group of intermediate **I** could be deprotonated, followed by the intramolecular 1,6-conjugate addition with an energy barrier of 21.6 kcal/mol (transition state K-TS). The final nine-membered heterocycle product **L** is formed through this reaction pathway.

We also conducted the DFT calculations for the [4 + 3] cycloaddition reaction between a simplified *p*-QM **SA3** and unsubstituted VEC **SA2** (Fig. 2). Similar to phenyl substituted VEC **SA1**, the cyclic carbonate **SA2** undergoes oxidative cleavage and CO2 extrusion to form the intermediate **D'**, with the energy barriers of 17.7 kcal/mol and 5.1 kcal/mol, respectively. After the *p*-QM **SA3** transfers the proton to the anionic oxygen center of **D'**, the nucleophilic nitrogen from **SA3** can attack the C5 or C3 position of the η^3-Pd-allyl species. In contrast to the energy profile in Fig. 1, the attack on the internal C3 position has the lowest energy barrier of 11.1 kcal/mol when unsubstituted VEC **SA2** was used here. The nucleophilic attack on the terminal carbon (C5 position) has a higher activation barrier (13.6 kcal/mol), which is kinetically unfavored. Next, the DBU promotes the intramolecular 1,6-conjugate addition reaction with the energy barrier of 17.6 kcal/mol and gives the seven-membered heterocycle product **L'**. The DFT calculations demonstrated that the regioselectivity was determined by the nucleophilic attack step (**E** to **F** and **E'** to **G'**). When phenyl substi-

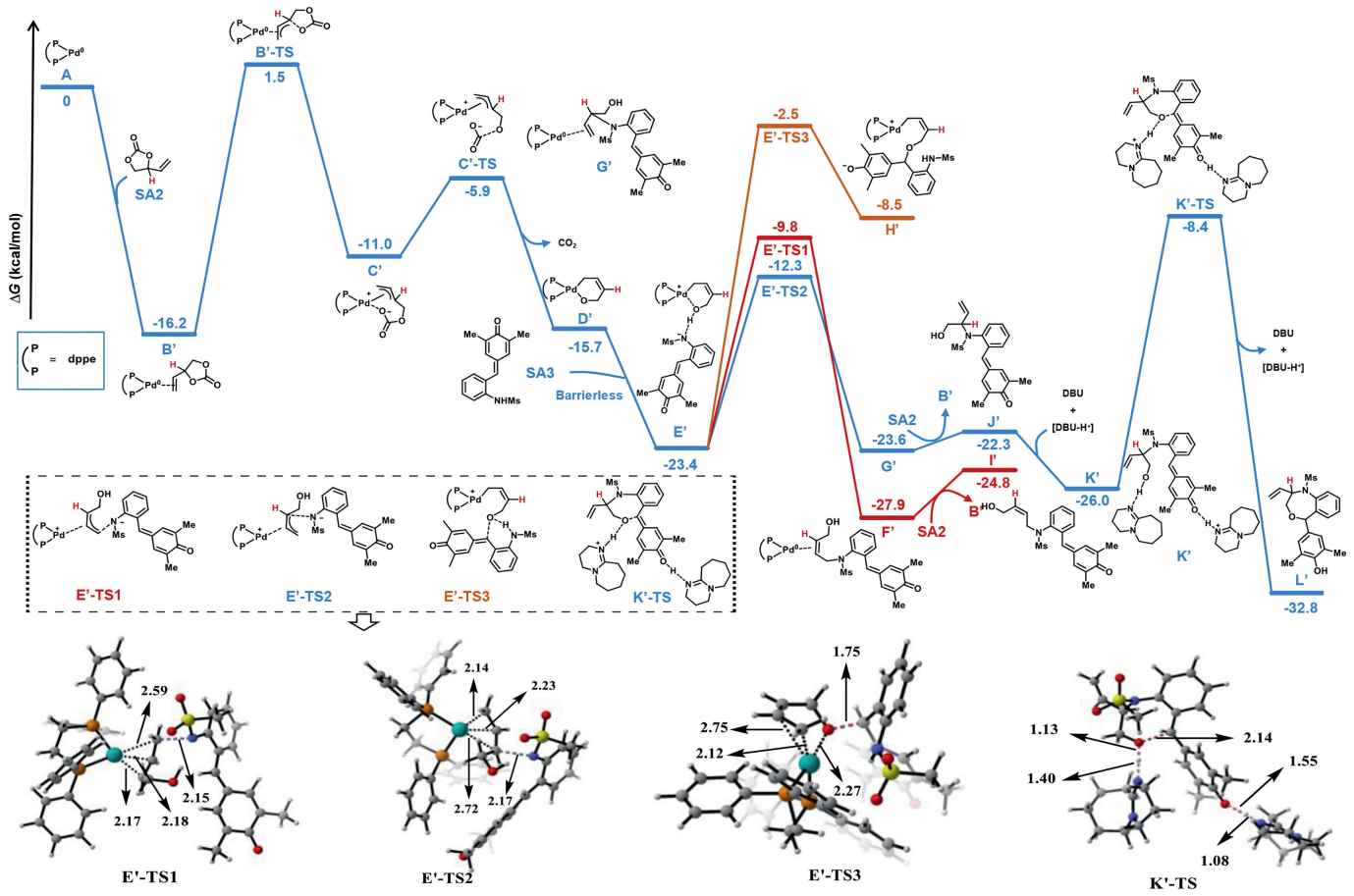

Fig. 2. DFT-computed energy profiles for the [4 + 3] cycloaddition of **SA3** and VEC **SA1**. Free energies in solution (in kcal/mol) at the SMD(toluene)-M06/Def2-TZVPP//PBE/SDD(Pd)/Def2-SVP (other atoms) level are displayed. DFT optimized geometries of selected transition states are shown. Bond lengths are in Å.

Table 2
Single point energies, distortion energies, and interaction energies for distortion/interaction analysis. Single point energies (in kcal/mol) at the SMD(toluene)-M06/Def2-TZVPP level are displayed.

Transition state	ΔE	ΔE_{dist}	ΔE_{int}
VEC = **SA1**			
E-TS1	13.0	51.4	−38.4
E-TS2	18.6	61.3	−42.6
$\Delta\Delta E$	5.6	9.9	−4.2
VEC = **SA2**			
E'-TS1	14.3	50.9	−36.6
E'TS2	10.3	49.7	−39.4
$\Delta\Delta E$	−4.0	−1.2	−2.8

tuted VEC **SA1** was used, the attack on the terminal position of the η^3-allylic group was kinetically favored. In contrast, when unsubstituted VEC **SA2** was employed, the attack on the internal position has the lowest energy barrier. These DFT computational results were in accordance with experimentally observed regioselectivity of those switchable cycloadditions of **1a** and **2**.

To gain a clearer understanding of the origin of the regioselectivity controlled by the VEC subrates (**SA1** and **SA2**), we performed the distortion/interaction analysis [63] of the nucleophilic attack transition states (Table 2). The contributions of distortion and interaction were calculated as follows:

$$\Delta E_{dist} = \left[E_{fragment\ D\text{or}\mathbf{D'}} + E_{fragment\ SA3}\right] - E_{E\ or\ \mathbf{E'}} \quad (1)$$

$$\Delta E_{\text{int}} = \Delta E_{TS} - \Delta E_{dist} \quad (2)$$

Our analysis indicated that the distortion energy is mostly responsible for the regioselectivity. For both VECs, the internal C3 position attacks have a higher interaction energy ($\Delta\Delta E_{\text{int}}$ = −4.2 kcal/mol and −2.8 kcal/mol, respectively). However, when phenyl substituted VEC **SA1** is employed, the internal C3 position attack (**E-TS2**) has a significantly greater distortion energy (61.3 kcal/mol), which could be a result of the phenyl group's steric effect on the **SA1** (see structures of **E-TS1** and **E-TS2** in Fig. 1).

Based on our preliminarily control experiments and computational results, we proposed a plausible mechanism that is same to the description of the computational study (Fig. 3).

In summary, we have successfully developed a regiodivergent cycloaddition of VECs with *p*-QMs. This transformation provides a highly selective protocol to rapidly access a wide range of medium-sized heterocycles. The substituents of VECs are found to be critical to obtain high regioselectivity, and by changing the steric properties of the substituents we could achieve either [4 + 5] or [4 + 3] cycloaddition reactions, affording nine- or seven-membered benzo-fused heterocycles which cannot be readily synthesized using the previous methods. In addition, this protocol is characterized by a broad substrate scope and excellent regioselectivity. Moreover, this method could be extended to the synthesis of eight- and ten-membered heterocycles. Control experiments supported that this switchable cycloaddition reaction proceeds in a domino fashion, the triggered step involves an intermolecular *N*-allylic substitution, followed by 1,6-conjugate addition reaction. The DFT calculation revealed that the steric hindrance of the substituent on vinyl carbamates is the key factor that account for the regioselectivity.

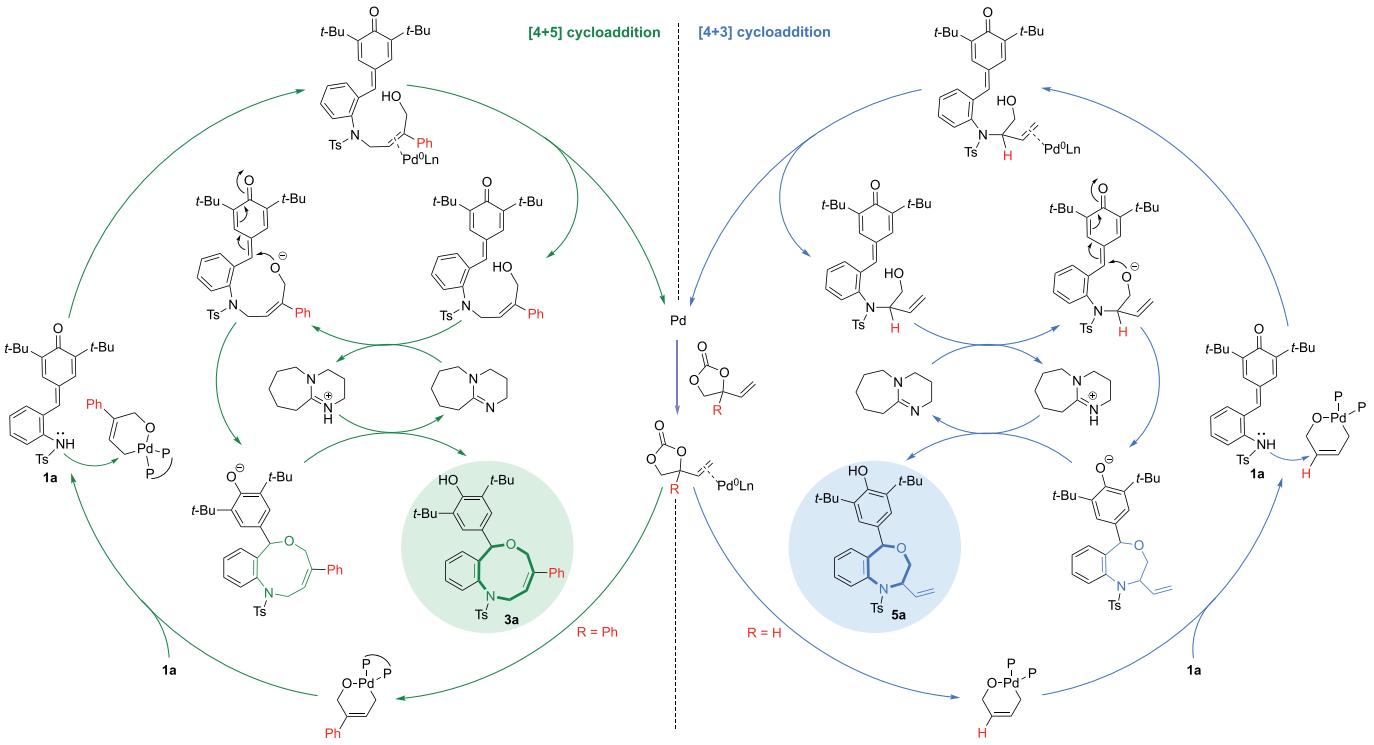

Fig. 3. Proposed mechanism.

Declaration of competing interest

The authors declare no conflict of interest.

Acknowledgments

This work was supported by the National Natural Science Foundation of China (Nos. 82173664, 81803342), "ShuangChuang" Research Team of Jiangsu Province (No. 20182036). C. Zhu acknowledges King Abdullah University of Science and Technology (KAUST) for support and the KAUST Supercomputing Laboratory for providing computational resources of the supercomputer Shaheen II.

Supplementary materials

Supplementary material associated with this article can be found, in the online version, at doi:10.1016/j.cclet.2022.01.063.

References

[1] A. Hussain, S.K. Yousuf, D. Mukherjee, RSC Adv. 4 (2014) 43241–43257.
[2] L. Yet, Chem. Rev. 100 (2000) 2963–3008.
[3] T. Miki, M. Kori, H. Mabuchi, et al., J. Med. Chem. 45 (2002) 4571–4580.
[4] R.A. Edrada, M. Heubes, G. Brauers, et al., J. Nat. Prod. 65 (2002) 1598–1604.
[5] Y. Nakagawa, K. Irie, Y. Nakamura, H. Ohigashi, Bioorg. Med. Chem. Lett. 11 (2001) 723–728.
[6] G. Illuminati, L. Mandolini, Acc. Chem. Res. 14 (2002) 95–102.
[7] S.K. Chattopadhyay, S. Karmakar, T. Biswas, et al., Tetrahedron 63 (2007) 3919–3952.
[8] V. Mahajan, H.J. Gais, Chem. Eur. J. 17 (2011) 6187–6195.
[9] M.E. Maier, Angew. Chem. Int. Ed. 39 (2000) 2073–2077.
[10] C.V.T. Vo, M.U. Luescher, J.W. Bode, Nat. Chem. 6 (2014) 310–314.
[11] C. Zhao, X. Xie, S. Duan, et al., Angew. Chem. Int. Ed. 53 (2014) 10789–10793.
[12] C. Guo, B. Sahoo, C.G. Daniliuc, F. Glorius, J. Am. Chem. Soc. 136 (2014) 17402–17405.
[13] H. Ni, X. Tang, W. Zheng, et al., Angew. Chem. Int. Ed. 56 (2017) 14222–14226.
[14] J.R. Donald, W.P. Unsworth, Chem. Eur. J. 23 (2017) 8780–8799.
[15] C.J. Roxburgh, Tetrahedron 49 (1993) 10749–10784.
[16] A. Khan, Y.J. Zhang, Synlett 26 (2015) 853–860.
[17] W. Guo, J.E. Gómez, Àlex. Cristòfol, J. Xie, A.W. Kleij, Angew. Chem. Int. Ed. 57 (2018) 13735–13747.
[18] Q.Z. Li, Y. Liu, M.Z. Li, et al., Org. Biomol. Chem. 18 (2020) 3638–3648.
[19] X. Wei, D. Liu, Q. An, Org. Lett. 17 (2015) 5768–5771.
[20] W. Guo, L. Martínez-Rodríguez, R. Kuniyil, et al., J. Am. Chem. Soc. 138 (2016) 11970–11978.
[21] W. Guo, L. Martínez-Rodríguez, E. Martin, E.C. Escudero-Adán, A.W. Kleij, Angew. Chem. Int. Ed. 55 (2016) 11037–11040.
[22] N. Miralles, J.E. Gómez, A.W. Kleij, E. Fernández, Org. Lett. 19 (2017) 6096–6099.
[23] J. Xie, W. Guo, A. Cai, E.C. Escudero-Adán, A.W. Kleij, Org. Lett. 19 (2017) 6388–6391.
[24] À. Cristòfol, E.C. Escudero-Adán, A.W. Kleij, J. Org. Chem. 83 (2018) 9978–9990.
[25] L. Deng, A.W. Kleij, W. Yang, Chem. Eur. J. 24 (2018) 19156–19161.
[26] A. Khan, J. Zhang, S. Khan, Green Chem. 22 (2020) 4116–4120.
[27] Y.J. Zhang, J.H. Yang, S.H. Kim, M.J. Krische, J. Am. Chem. Soc. 132 (2010) 4562–4563.
[28] W. Guo, L. Martínez-Rodríguez, R. Kuniyil, et al., J. Am. Chem. Soc. 138 (2016) 11970–11978.
[29] A. Khan, S. Khan, I. Khan, et al., J. Am. Chem. Soc. 139 (2017) 10733–10741.
[30] A. Khan, R. Zheng, Y. Kan, et al., Angew. Chem. Int. Ed. 53 (2014) 6439–6442.
[31] A. Khan, L. Yang, J. Xu, L.Y. Jin, Y.J. Zhang, Angew. Chem. Int. Ed. 53 (2014) 11257–11260.
[32] A. Khan, J.X. Xing, J.M. Zhao, et al., Chem. Eur. J. 21 (2015) 120–124.
[33] L. Yang, A. Khan, R.F. Zheng, L.Y. Jin, Y.J. Zhang, Org. Lett. 17 (2015) 6230–6233.
[34] K. Liu, I. Khan, J. Cheng, Y.J. Hsueh, Y.J. Zhang, ACS Catal. 8 (2018) 11600–11604.
[35] J. Wang, L. Zhao, Q. Rong, et al., Org. Lett. 22 (2020) 5833–5838.
[36] Z.Q. Rong, L.C. Yang, S. Liu, et al., J. Am. Chem. Soc. 139 (2017) 15304–15307.
[37] P. Das, S. Gondo, P. Nagender, et al., Chem. Sci. 9 (2018) 3276–3281.
[38] H. Uno, N. Punna, E. Tokunaga, M. Shiro, N. Shibata, Angew. Chem. Int. Ed. 59 (2020) 8187–8194.
[39] Y. Wei, S. Liu, M.M. Li, et al., J. Am. Chem. Soc. 141 (2019) 133–137.
[40] X. Zhang, X. Li, J.L. Li, et al., Chem. Sci. 11 (2020) 2888–2894.
[41] L.C. Yang, Z.Q. Rong, Y.N. Wang, et al., Angew. Chem. Int. Ed. 56 (2017) 2927-2927.
[42] L.C. Yang, Z.Y. Tan, Z.Q. Rong, et al., Angew. Chem. Int. Ed. 57 (2018) 7860–7864.
[43] H.W. Zhao, L.R. Wang, J.M. Guo, et al., Adv. Synth. Catal. 361 (2019) 4761–4771.
[44] R. Zeng, J.L. Li, X. Zhang, et al., ACS Catal. 9 (2019) 8256–8262.
[45] P. Chauhan, U. Kaya, D. Enders, Adv. Synth. Catal. 359 (2017) 888–912.
[46] J.Y. Wang, W.J. Hao, S.J. Tu, B. Jiang, Org. Chem. Front. 7 (2020) 1743–1778.
[47] W.D. Chu, L.F. Zhang, X. Bao, et al., Angew. Chem. Int. Ed. 52 (2013) 9229–9233.
[48] L. Caruana, F. Kniep, T.K. Johansen, P.H. Poulsen, K.A. Jørgensen, J. Am. Chem. Soc. 136 (2014) 15929–15932.
[49] Z. Wang, Y.F. Wong, J. Sun, Angew. Chem. Int. Ed. 54 (2015) 13711–13714.
[50] K. Zhao, Y. Zhi, A. Wang, D. Enders, ACS Catal. 6 (2016) 657–660.
[51] K. Zhao, Y. Zhi, T. Shu, et al., Angew. Chem. Int. Ed. 55 (2016) 12104–12108.
[52] Y. Zhi, K. Zhao, C. von Essen, K. Rissanen, D. Enders, Org. Chem. Front. 5 (2018) 1348–1351.
[53] J. Wang, X. Pan, J. Liu, et al., Org. Lett. 20 (2018) 5995–5998.

[54] J. Wang, X. Pan, L. Zhao, et al., Org. Biomol. Chem. 17 (2019) 10158–10162.
[55] J.P. Perdew, K. Burke, Phys. Rev. Lett. 77 (1996) 3865–3868.
[56] J.P. Perdew, K. Burke, M. Ernzerhof, et al., Phys. Rev. Lett. 78 (1998) 1396.
[57] F. Weigend, R. Ahlrichs, PCCP 7 (2005) 3297–3305.
[58] U. Haeusermann, M. Dolg, H. Stoll, H. Preuss, Mol. Phys. 78 (1993) 1211–1224.
[59] W. Kuechle, M. Dolg, H. Stoll, H. Preuss, J. Chem. Phys. 100 (1994) 7535–7542.
[60] T. Leininger, A. Nicklass, H. Stoll, M. Dolg, P. Schwerdtfeger, J. Chem. Phys. 105 (1996) 1052–1059.
[61] Y. Zhao, D.G. Truhlar, Theor. Chem. Acc. 120 (2008) 215–241.
[62] A.V. Marenich, C.J. Cramer, D.G. Truhlar, J. Phys. Chem. B 113 (2009) 6378–6396.
[63] F.M. Bickelhaupt, K.N. Houk, Angew. Chem. Int. Ed. 56 (2017) 10070–10086.